

Apsidal Motion in Massive Eccentric Binaries in NGC 6231

Sophie Rosu

Space sciences, Technologies and Astrophysics Research (STAR) Institute, Université de Liège, Allée du six Août, 19c, Bât B5c, 4000 Liège, Belgium

The young and rich open cluster NGC 6231 hosts a substantial population of O-type binary stars. We study several of these eccentric short-period massive eclipsing binaries and assess their fundamental parameters (e.g. masses, radii, effective temperatures, luminosities). To this aim, we use both spectroscopic and photometric observations of the systems.

The properties of these systems make them interesting targets to study tidally induced apsidal motion. The analysis of apsidal motion offers a powerful means to obtain information about the stellar interior, which is otherwise difficult to get. Indeed, since the rate of apsidal motion in a binary system is proportional to the internal structure constants (a global measure of the density contrast between the stellar core and external layers) of the stars composing it, its value gives direct insight into the internal structure and evolutionary state of these stars.

Stellar evolution models are constructed based on the observationally determined fundamental parameters and a theoretical rate of apsidal motion is inferred. The results are striking: adopting standard stellar evolution models yields a theoretical rate of apsidal motion much larger than the observational value. This discrepancy results from the standard models predicting too low an efficiency of internal mixing and thus too low a density contrast. By enforcing the theoretical rates of apsidal motion to match the observational values, enhanced mixing is required, through a large overshooting parameter and/or additional turbulent/rotational mixing. Our analysis leads to the conclusion that the convective cores in those massive stars must be more extended than anticipated from standard models.

Introduction

A crucial diagram in Astronomy is the Hertzsprung-Russell (HR) diagram, named after the Danish astronomer Ejnar Hertzsprung (1873-1967) and the American astronomer Henry Norris Russell (1877-1957). Several forms of this diagram exist: the original one displays the absolute visual magnitude of the stars as a function of its spectral type. The HR diagram shown in Figure 1 displays the luminosity of the star as a

function of its effective surface temperature in a log-log scale, and is the one usually used for theoretical calculations of stellar structure and evolution. The main feature of this diagram is that it can be used to illustrate the evolution of stars. The main diagonal in this diagram (from the hottest and most luminous O-type stars to the coolest and least luminous M-type stars) is populated by the stars located in their main-sequence phase. This is the longest phase of stellar evolution during which the stars are burning hydrogen

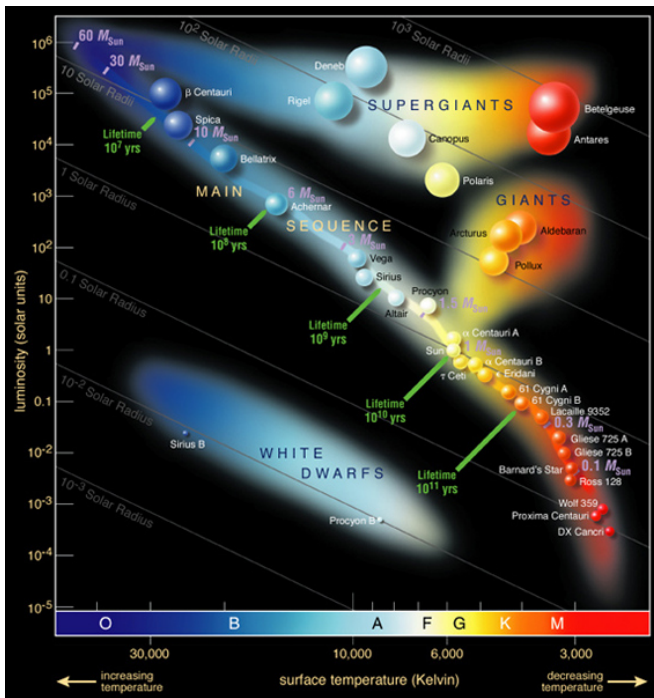


Figure 1: Hertzsprung-Russell diagram. © <http://omsj.info>.

in their core. When the stars evolve away from the main-sequence phase, two main evolutionary paths exist, depending on the initial mass of the stars. The more massive stars see their envelope expanding and their surface effective temperature decreases. As a consequence, they move towards the right side of the HR diagram. The temperature inside the core becomes sufficiently high to allow for Helium burning. The stars become red- and blue-giants and supergiants stars. The less massive stars progressively become red giants and their effective temperature decreases. At the end of its life, the core of the red giant collapses into a white dwarf, hence moving towards the left side of the HR diagram, while the remaining envelope forms a planetary nebula.

This paper aims at studying the massive stars, namely late O- and early B-type stars still on the main-sequence phase, and having a mass ranging between 9 and $30 M_{\odot}$. It appears that the majority of these massive stars belong to a binary system: they are bound by gravitational attraction to a companion [Sana et al., 2012, Duchêne et al., 2013]. This situation has important implications for the evolution of massive stars: Whilst the evolution of a single massive star is determined by its initial mass, its mass-loss rate, and its rotation

rate [Ekström et al., 2012, Brott et al., 2011], the evolution of a massive binary is considerably more complex and depends not only on the properties of the stars, but also on the parameters of the binary orbit [Wellstein et al., 2001]. Indeed, the stars in a binary system can exchange mass and angular momentum through tidal interactions and Roche lobe¹ overflow leading to a diversity of evolutionary sequences for both the mass gainer and the mass loser [Vanbeveren et al., 1998, Raucq et al., 2017]. Understanding the evolution of massive binaries is also of primary importance in the context of the detections of gravitational wave events with the LIGO and Virgo experiment [Abbott et al., 2016]. The events that have been reported so far were associated either with the coalescence of two stellar-mass black holes or of two neutron stars. In either case, the progenitors of these events were end products of the evolution of two very massive stars in a binary system [Kruckow et al., 2016]. Indeed, a massive star ends its life in a supernova explosion: Its envelope is vehemently expelled into the interstellar medium, enriching the latter in processed material, while the remaining stellar core collapses into either a neutron star or a black hole.

During earlier phases of stellar evolution, well before the extreme events of supernova explosion and mergers, we can already observe binary interactions: the tidal interactions. Tidal interactions lead to dynamical deformations of the shapes of the stars, which are therefore not spherically symmetric anymore [Moreno et al., 2011]. These deformations in turn induce secular changes of the orbital parameters, the most prominent effect being the slow precession of the line of apsides with time, known as the apsidal motion [Schmitt et al., 2016]. The line of apsides is the line joining the point of closest approach and the point of largest separation between the two stars (i.e. the major axis of the binary orbit). This motion takes its origin from the three-dimensional shape of the stars. Indeed, for point-like masses, the motion is purely Keplerian but, because of the three-dimensional extension of the stars, a Newtonian perturbation exists and the motion is non-Keplerian. The

¹ The Roche lobe is the region around the star in a binary system within which the material is gravitationally bound to that star.

apsidal motion is thence a Newtonian effect. In addition, a general relativistic correction coming from Einstein’s general relativity exists, which acts in the same direction as the Newtonian perturbation and is usually smaller than the Newtonian effect, except for some extreme cases, see e.g., [Baroch et al., 2021]. The rate of this apsidal motion is directly related to the internal structure of the stars that make up the binary system [Shakura, 1985]. Measuring the rate of apsidal motion hence provides a diagnostic of the otherwise difficult to constrain internal structure of stars, and offers a test of our understanding of stellar structure and evolution [Claret & Giménez, 2010].

The binary systems which the present study focuses on belong to the young open cluster NGC 6231 located in the core of the Scorpius OB1 association. This cluster hosts a substantial population of O- and B-type stars at its core, a large fraction of which were found to belong to binary systems [Sana et al., 2008]. Those systems, due to their properties, are interesting targets to study tidally induced apsidal motion [Rosu et al., 2020a, Rosu et al., 2020b, Rosu et al., 2022].

Measuring the apsidal motion rate

Two main methods exist to determine the apsidal motion rate of a binary system from observations, depending on whether the binary system under consideration is an eclipsing binary system for which photometric observations are available (see e.g. [Zasche & Wolf, 2019, Baroch et al., 2021]) or it is a spectroscopic binary system for which radial velocity measurements of the components are available (see e.g. [Rauw et al., 2016, Rosu et al., 2020a]). The radial velocities are the velocities of the stars projected onto our line-of-sight, changing in time as the stars orbit one another. In the present context, we focus on binary systems that are both spectroscopic and eclipsing systems. The procedure we follow consists in three major steps.

In a first step, the spectroscopic observations of the binary system are analysed. If only the lines of the primary star, usually the most luminous and massive star of the binary system, are seen in the

spectra, then the binary is called an SB1 system. On the opposite, if both the lines belonging to the primary and secondary stars are seen in the spectra, then the binary system is called an SB2 system. For the latter one, it is first necessary to disentangle the contributions of the two stars. This is done using a disentangling method (described in [González & Levato, 2006]): The code takes all the spectroscopic observations as input, and gives, as output, both the separate spectra of the individual components and the radial velocities of both stars at each time of observation. The individual spectra are then further analysed by means of non-local thermodynamic model atmosphere codes such as CMFGEN [Hillier & Miller, 1998] to assess the effective temperature and the surface gravity of the stars, notably (see Figure 2).

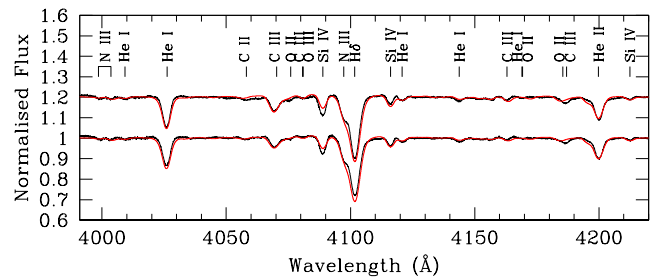


Figure 2: CMFGEN ajustement (in red) of the primary and secondary spectra (in black) of the binary system HD 152248. Note that the secondary spectrum has been shifted by +0.2 in the y-axis for convenience.

In a second step, the radial velocities are fit according to the following equation

$$RV(t) = K (\cos(\phi(t) + \omega(t)) + e \cos(\omega(t))) + \gamma, \tag{1}$$

where K is the semi-amplitude of the radial velocity curve, γ is the apparent systemic velocity of the system (i.e. its velocity with respect to the observer), e is the eccentricity of the system, ω is the argument of periastron, and ϕ is the true anomaly (see Figure 3). This expression explicitly accounts for apsidal motion in the system inasmuch as the argument of periastron ω is assumed to linearly vary with time through the following expression

$$\omega(t) = \omega_0 + \dot{\omega}(t - T_0), \tag{2}$$

where $\dot{\omega}$ is the apsidal motion rate and ω_0 is the argument of periastron at the time of reference T_0 . An example of radial velocity adjustment is shown in Figure 4 for the binary system HD 152219. As the

apsidal motion is a slow precession, we stress here that observations spanning several years, or even decades, are usually necessary to get an accurate measure of the apsidal motion rate of a system; this is a restricting condition to the number of systems for which apsidal motion can be studied.

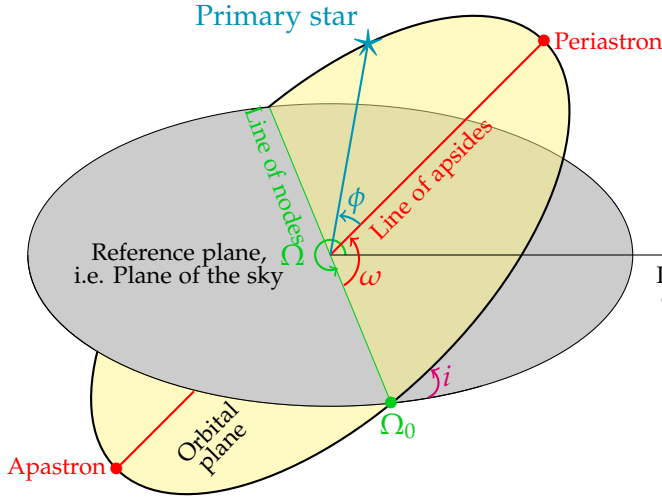


Figure 3: Definition of the orbital elements of a binary system.

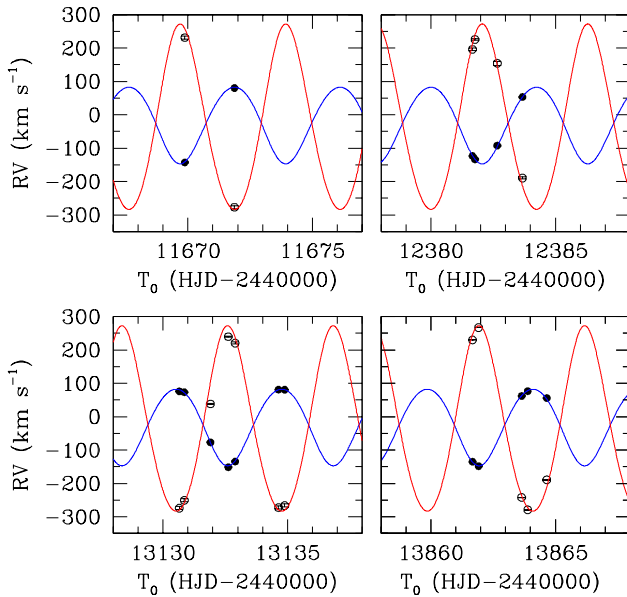


Figure 4: Measured radial velocities of the primary (filled dots) and secondary (open dots) stars of the massive binary HD 152219, and radial velocity curves obtained with the best-fit parameters (in blue and red for the primary and secondary stars, respectively). Data from [Rosu et al., 2022].

In a third step, the photometric observations of the system are analysed: The light curves are fit with codes such as *Nightfall* [Wichmann, 2011] (see Figure 5) that allow us to determine the inclination of the system and the masses and radii

of the stars, notably. We note that the light curves of a binary system can also be used to assess the apsidal motion rate of a binary system if photometric observations exist for several epochs. Indeed, the shape of the light curve changes in time, and we refer to [Rosu, 2021] for detailed information.

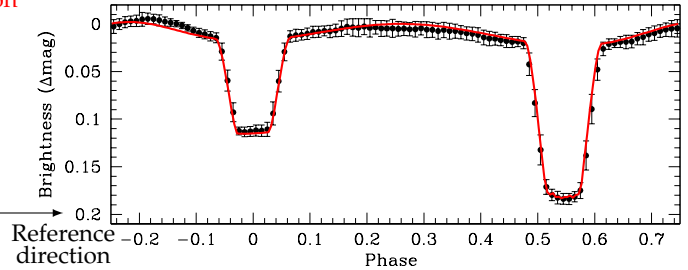


Figure 5: Best-fit *Nightfall* solution (in red) of the light curve of the binary system HD 152219 (in black).

Sounding the interior of massive stars

The apsidal motion rate of a binary system is made of two contributions – the Newtonian contribution (N) and the general relativistic correction (GR) –, as mentioned in the introduction:

$$\dot{\omega} = \dot{\omega}_N + \dot{\omega}_{GR}. \quad (3)$$

The general relativistic correction takes the form given by [Shakura, 1985]:

$$\dot{\omega}_{GR} = \left(\frac{2\pi}{P_{orb}} \right)^{5/3} \frac{3(G(M_1 + M_2))^{2/3}}{c^2(1 - e^2)}, \quad (4)$$

when only the quadratic corrections are taken into account. In this expression, G and c stand for the gravitational constant and the speed of light, respectively. P_{orb} and e are the orbital period and the eccentricity of the system, respectively, while M_1 and M_2 are the masses of the primary and secondary stars, respectively.

The Newtonian contribution takes the form given by [Sterne, 1939], if the stellar rotation axes are orthogonal to the orbital plane and where only the dominant contributions arising from the second-order harmonic distortions of the potential

are considered:

$$\dot{\omega}_N = \frac{2\pi}{P_{\text{orb}}} \left[15f(e) \left\{ k_{2,1q} \left(\frac{R_1}{a} \right)^5 + \frac{k_{2,2}}{q} \left(\frac{R_2}{a} \right)^5 \right\} + g(e) \left\{ k_{2,1}(1+q) \left(\frac{R_1}{a} \right)^5 \left(\frac{P_{\text{orb}}}{P_{\text{rot},1}} \right)^2 + k_{2,2} \frac{1+q}{q} \left(\frac{R_2}{a} \right)^5 \left(\frac{P_{\text{orb}}}{P_{\text{rot},2}} \right)^2 \right\} \right] \quad (5)$$

where $q = \frac{M_2}{M_1}$ is the mass ratio of the system, R_1 and R_2 are the radii of the primary and secondary stars, respectively, $P_{\text{rot},1}$ and $P_{\text{rot},2}$ are the rotational periods of the primary and secondary stars, respectively, and a is the semi-major axis of the system. $f(e)$ and $g(e)$ are two functions of the eccentricity given by

$$\begin{cases} f(e) = \frac{1 + \frac{3e^2}{2} + \frac{e^4}{8}}{(1-e^2)^5}, \\ g(e) = \frac{1}{(1-e^2)^2}. \end{cases} \quad (6)$$

Finally, $k_{2,1}$ and $k_{2,2}$ are the internal structure constants of the primary and secondary stars, respectively. The internal structure constant k_2 , also known as the apsidal motion constant, is expressed as

$$k_2 = \frac{3 - \eta_2(R_*)}{4 + 2\eta_2(R_*)}, \quad (7)$$

where

$$\eta_2(R_*) = \left. \frac{d \ln \epsilon_2}{d \ln r} \right|_{r=R_*} \quad (8)$$

is the logarithmic derivative of the surface harmonic of the distorted star evaluated at the stellar surface ($r = R_*$), expressed in terms of the ellipticity ϵ_2 . $\eta_2(R_*)$ is the solution of the Clairaut-Radau differential equation

$$r \frac{d\eta_2(r)}{dr} + \eta_2^2(r) - \eta_2(r) + 6 \frac{\rho(r)}{\bar{\rho}(r)} (\eta_2(r) + 1) - 6 = 0 \quad (9)$$

with the boundary condition $\eta_2(0) = 0$ [Hejlesen, 1987]. The terms $\rho(r)$ and $\bar{\rho}(r)$ are the density at distance r from the centre of the star and the mean density within the sphere of radius r . The apsidal motion constant is a measure of the internal mass distribution of the star, that is to say of the density contrast between the core and the external layers of the star. k_2 takes its maximum value of 0.75 for a homogeneous sphere

and its value can decrease towards values as low as 10^{-4} for massive stars having a dense core and a diluted envelope [Rosu et al., 2020b]. During its evolution, the core of the star becomes denser and denser while its envelope becomes more and more diluted, thence k_2 decreases with time, rendering this quantity a good indicator of stellar evolution.

All quantities appearing in Equations 4 and 5, except for $k_{2,1}$ and $k_{2,2}$, can be determined from observations. Hence, we are left with an underdetermined system, unless the binary system is a twin system, in which case the two stars are identical and share the same physical properties. Twin system are rather scarce – the binary HD 152248 discussed below is one of them – and offer a unique opportunity to observationally constrain the k_2 -value [Rosu et al., 2020b]. In the general case, we can rewrite Equation 5 in the form

$$\dot{\omega} = c_1 k_{2,1} + c_2 k_{2,2}, \quad (10)$$

and further define a weighted-average mean of the internal structure constants of the stars

$$\bar{k}_2 = \frac{c_1 k_{2,1} + c_2 k_{2,2}}{c_1 + c_2} = \frac{\dot{\omega}}{c_1 + c_2}, \quad (11)$$

that is entirely determined from observations, as all terms appearing in the right-hand side are.

This observational quantity can further be compared to the one obtained based on stellar structure and evolution models. A stellar evolution model is a numerical model following the evolution of the star and its fundamental properties with time from its birth to advanced stages of its evolution. To first order, the interior of a massive star consists of a convective core and a radiative envelope, differing by the mode of transfer of the energy. In stellar evolution models for massive stars, two ingredients are added to this general framework: semi-convection and turbulent diffusion. Semi-convection arises from the fact that the elements in the convective core, due to their inertia, do not stop at the border between the convective core and the radiative envelope, but continue to move in a certain region of the radiative zone, called the semi-convective region. The thickness of this region is given by the step-function

$$d_{\text{ov}} = \alpha_{\text{ov}} \min(H_p(r_c), h), \quad (12)$$

where h is the thickness of the convective zone, $H_p(r_c)$ is the pressure scale height (ratio between the pressure and the product between the density and the local gravity) evaluated at the edge of the convective core, and α_{ov} is the overshooting parameter. This latter is poorly constrained, but should be equal to or greater than 0.20 for massive stars (see e.g., [Claret & Torres, 2019]). Turbulent diffusion is responsible for the transport of processed material from the core to the external layers and for the transport of hydrogen from the external layers to the core. The turbulent diffusion is implemented as a diffusion term added to the velocity of the considered element and acts as reducing the abundance gradient of the element. It is parameterised by the turbulent coefficient D_T measured in $\text{cm}^2 \text{s}^{-1}$. Both mechanisms increase the size of the convective core by bringing additional hydrogen, that is to say fuel for nuclear reactions, and, therefore, increase the lifetime of the star on its main-sequence phase.

Binary systems in NGC 6231

The methodology presented in the previous sections has been successfully applied to two massive eccentric binary systems belonging to the young open cluster NGC 6231, namely HD 152248 and HD 152219. The former system is a twin system: the two components are identical, that is to say they have the same mass, radius, effective temperature, and luminosity. By contrast, HD 152219 is made of a primary star bigger and more massive than the secondary companion. We proceeded identically for the two systems to determine their observational properties, which are summarised in Table 1. In the case of HD 152248, as the two stars are identical, their internal structure constants are both equal to the mean value \bar{k}_2 . We here focus on the stellar evolution models constructed with the C1és code (Code Liégeois d'Évolution Stellaire [Scuflaire et al., 2008]) for both binary systems to reproduce their physical parameters.

HD 152248

Given that the binary system is a twin system, we only need to build a single model that will represent the two stars. In a first attempt to reproduce the physical properties of the stars, namely their masses

Table 1: Set of observationally-determined properties of the binary systems HD 152248 and HD 152219.

Parameter	Value	
	HD 152248	HD 152219
$M (M_\odot)$	$29.5^{+0.5}_{-0.4}$	18.64 ± 0.47
	$29.5^{+0.5}_{-0.4}$	7.70 ± 0.12
$R (R_\odot)$	$15.07^{+0.08}_{-0.12}$	9.40 ± 0.15
	$15.07^{+0.08}_{-0.12}$	3.69 ± 0.06
$T_{\text{eff}} (\text{K})$	$34\,000 \pm 1000$	$30\,900 \pm 1000$
	$34\,000 \pm 1000$	$21\,700 \pm 1000$
$L_{\text{bol}} (L_\odot)$	$(2.73 \pm 0.32) \times 10^5$	$(7.26 \pm 0.97) \times 10^4$
	$(2.73 \pm 0.32) \times 10^5$	$(2.73 \pm 0.51) \times 10^3$
\bar{k}_2	0.0010 ± 0.0001	0.00173 ± 0.00052
$\dot{\omega} (^\circ \text{yr}^{-1})$	$1.843^{+0.064}_{-0.083}$	1.198 ± 0.300

and their positions in the HR diagram only, we built a first best-fit model with an overshooting parameter $\alpha_{ov} = 0.20$ and no turbulent diffusion. The evolutionary track corresponding to this best-fit model is plotted in blue in Figure 6 together with the observational value and its error bars (in red). We observe that this model is not able to reproduce the physical properties of the stars.

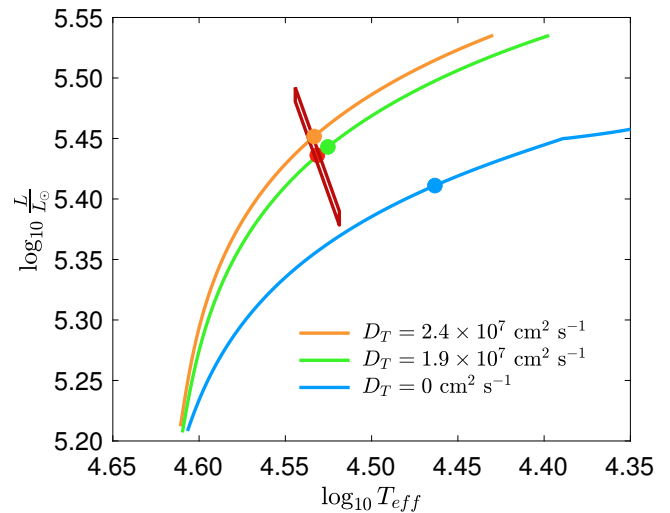


Figure 6: Hertzsprung-Russell diagram for HD 152248: evolutionary tracks of C1és models. The dots over-plotted on the tracks correspond to the models that fit the observational k_2 . The observational value and its error bars are represented in red.

We then allowed for the turbulent diffusion to take a non-zero value and found a best-fit model having a turbulent diffusion characterised by $D_T = 1.9 \times 10^7 \text{cm}^2 \text{s}^{-1}$ and able to reproduce the physical properties of the stars, namely their mass,

radius, and position in the HR diagram. The track corresponding to this best-fit model is plotted in green in Figure 6. However, we observe that the model having the correct k_2 -value, symbolised by the dot over-plotted on the track, is located further away on the evolutionary track compared to the location of the best-fit model. Remembering that the internal structure constant decreases with time as the star evolves, this means that the best-fit model has too high a k_2 -value, that is to say too low a density contrast between the stellar core and the envelope, and the star is too homogenous in terms of mass distribution.

To overcome this difficulty, we enforced some turbulent diffusion inside the model and found a model that is able to fit not only the mass, radius, and position in the HR diagram, but also the k_2 -value and the apsidal motion rate. This best-fit model has an enhanced turbulent diffusion coefficient $D_T = 2.4 \times 10^7 \text{ cm}^2 \text{ s}^{-1}$ and is plotted in orange in Figure 6. This result is valuable, in the sense that it shows that without taking into account the apsidal motion occurring in this binary system, we would not highlight that the standard models predict a too low density contrast compared to what is expected from observations. This enhanced turbulent diffusion might come from mixing induced by stellar rotation, as suggested by [Rosu et al., 2020b].

HD 152219

In the case of HD 152219, from the weighted-average mean of the internal structure constants of the two stars, \bar{k}_2 , and the fact that the primary star is the most massive object, and so the more evolved one, we deduce that $k_{2,1} \leq \bar{k}_2 \leq k_{2,2}$. Thanks to the analysis performed for HD 152248, we expect that this relation puts a constraint on the internal structure constant of the primary star: The standard stellar evolution models of the primary star predict too low a density contrast inside the star when a best-fit model of the mass, radius, and position in the HR diagram is considered, as indicated in green in Figure 7.

We hence proceeded as previously and searched for a best-fit model of the afore-mentioned quantities and of the internal structure constant, adopting the least stringent constraint on $k_{2,1}$,

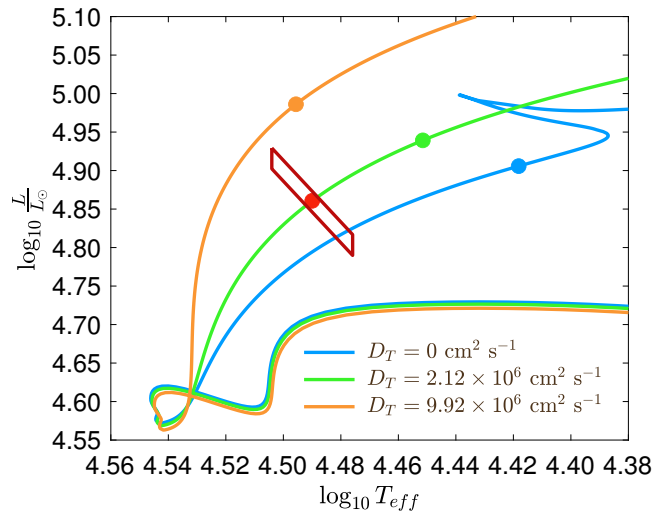


Figure 7: Hertzsprung-Russell diagram for HD 152219: evolutionary tracks of *Ciés* models. The dots over-plotted on the tracks correspond to the models that fit the observational \bar{k}_2 . The observational value and its error bars are represented in red.

namely enforcing $k_{2,1} = \bar{k}_2$. The evolutionary track corresponding to the best-fit model obtained in this way is plotted in orange in Figure 7. Even though the discrepancy in k_2 is lowered, we observe that the best-fit model does not reproduce the position in the HR diagram anymore. We expect this difference to come from the high stellar rotational period that could induce additional rotational mixing. One way to infirm or confirm this statement would be to build stellar evolution models with the GENEC code accounting for the mixing induced by stellar rotation.

Conclusion

From a set of observational data of a binary system, namely spectroscopic, photometric, and radial velocities measurements, we can not only determine the fundamental properties of the stars such as their masses, radii, effective temperatures, and luminosities, but also the physical properties of the binary system such as the eccentricity and the inclination of the orbit, the orbital period of the system, and most importantly in the context of this study, the apsidal motion rate $\dot{\omega}$ of the system. Thanks to the apsidal motion rate determination, we can sound the interior of massive stars through the internal structure constant k_2 appearing in the theoretical expression of $\dot{\omega}$.

We can further build stellar evolution models to be confronted to the observational stellar parameters. We put stringent constraints on the standard stellar evolution models: These models predict too low a density contrast between the core and the external layers of the stars compared to what is expected from the observations. To solve this issue, enhanced mixing, either through overshooting and/or turbulent diffusion and/or rotational mixing, needs to be included inside the models. This additional mixing introduced into the model has the impact of increasing the stellar core size and extending the main-sequence phase of the star.

Acknowledgments

This work is supported by the Fonds de la Recherche Scientifique (F.R.S. - FNRS, Belgium). I thank Gregor Rauw for his suggestions towards the improvement of the manuscript.

References

- [Abbott et al., 2016] Abbott, B. P., Abbott, R., Abbott, T. D., et al. (2016). Observation of Gravitational Waves from a Binary Black Hole Merger. *Phys. Rev. Letters*, 116:061102.
- [Baroch et al., 2021] Baroch, D., Giménez, A., Ribas, I., et al. (2021). Analysis of apsidal motion in eclipsing binaries using TESS data. I. A test of gravitational theories. *A&A*, 649:A64.
- [Brott et al., 2011] Brott, I., de Mink, S. E., Cantiello, M., et al. (2011). Rotating massive main-sequence stars. I. Grids of evolutionary models and isochrones. *A&A*, 530:A115.
- [Claret & Giménez, 2010] Claret, A., & Giménez, A. (2010). The apsidal motion test of stellar structure and evolution: an update. *A&A*, 519:A57.
- [Claret & Torres, 2019] Claret, A., & Torres, G. (2019). The Dependence of Convective Core Overshooting on Stellar Mass: Reality Check and Additional Evidence. *ApJ*, 876:134.
- [Duchêne et al., 2013] Duchêne, G., & Kraus, A. (2013). Stellar multiplicity. *ARA&A*, 51:269.
- [Ekström et al., 2012] Ekström, S., Georgy, C., Eggenberger, P., et al. (2012). Grids of stellar models with rotation. I. Models from 0.8 to 120 M_{\odot} at solar metallicity ($Z=0.014$). *A&A*, 537:A146.
- [González & Levato, 2006] González, J. F., & Levato, H. (2006). Separation of composite spectra: the spectroscopic detection of an eclipsing binary star. *A&A*, 448:283.
- [Hejlesen, 1987] Hejlesen, P. M. (1985). Studies in stellar evolution. III - The internal structure constants. *A&AS*, 69:251.
- [Hillier & Miller, 1998] Hillier, J. D., & Miller, D. L. (1998). The Treatment of Non-LTE Line Blanketing in Spherically Expanding Outflows. *ApJ*, 496:407.
- [Kruckow et al., 2016] Kruckow, M. U., Tauris, T. M., Langer, N., et al. (2016). Common-envelope ejection in massive binary stars. Implications for the progenitors of GW150914 and GW151226. *A&A*, 596:A58.
- [Moreno et al., 2011] Moreno, E., Koenigsberger, G., & Harrington, D. M. (2011). Eccentric binaries. Tidal flows and periastron events. *A&A*, 528:A48.
- [Raucq et al., 2017] Raucq, F., Gosset, E., Rauw, G., et al. (2017). Observational signatures of past mass-exchange episodes in massive binaries: the case of LSS3074. *A&A*, 601:A133.
- [Rauw et al., 2016] Rauw, G., Rosu, S., Noels, A., et al. (2016). Apsidal motion in the massive binary HD 152218. *A&A*, 594:A33.
- [Rosu et al., 2020a] Rosu, S., Rauw, G., Conroy, K. E., et al. (2020). Apsidal motion in the massive binary HD 152248. *A&A*, 635:145.
- [Rosu et al., 2020b] Rosu, S., Noels, A., Dupret, M.-A., et al. (2020). Apsidal motion in the massive binary HD 152248. Constraining the internal structure of the stars. *A&A*, 642:221.
- [Rosu, 2021] Rosu, S. (2021). What apsidal motion reveals about the interior of massive stars. *Bulletin de la Société Royale des Sciences de Liège*, 90:1.

- [Rosu et al., 2022] Rosu, S., Rauw, G., Farnir, M., Dupret, M.-A., & Noels, A. (2022). Apsidal motion in massive eccentric binaries in NGC 6231. The case of HD 152219. *A&A*, in press [arXiv:2202.02012].
- [Sana et al., 2012] Sana, H., de Mink, S. E., de Koter, A., et al. (2012). Binary Interaction dominates the Evolution of Massive Stars. *Science*, 337:444.
- [Sana et al., 2008] Sana, H., Gosset, E., Nazé, Y., Rauw, G., & Linder, N. (2008). The massive star binary fraction in young open clusters – I. NGC 6231 revisited. *MNRAS*, 386:447.
- [Schmitt et al., 2016] Schmitt, J. H. M. M., Schröder, K.-P., Rauw, G., et al. (2016). The α CrB binary system: A new radial velocity curve, apsidal motion, and the alignment of rotation and orbit axes. *A&A*, 586:A104.
- [Scuflaire et al., 2008] Scuflaire, R., Théado, S., Montalbán, J., et al. (2008). CLÉS, Code Liégeois d'Évolution Stellaire. *Ap&SS*, 316:83.
- [Shakura, 1985] Shakura, N. I. (1985). On the Apsidal Motion in Binary Stars. *Sov. Astron. Lett.*, 11:224.
- [Sterne, 1939] Sterne, T. E. (1939). Apsidal motion in binary stars. *MNRAS*, 99:451.
- [Vanbeveren et al., 1998] Vanbeveren, D., De Loore, C., & Van Rensbergen, W. (1998). Massive Stars. *A&ARv*, 9:63.
- [Wellstein et al., 2001] Wellstein, S., Langer, N., & Braun, H. (2001). Formation of contact in massive close binaries. *A&A*, 369:939.
- [Wichmann, 2011] Wichmann, R. (2011). Astrophysics Source Code Library. [record ascl:1106.016].
- [Zasche & Wolf, 2019] Zasche, P., & Wolf, M. (2019). Apsidal Motion and Absolute Parameters of 21 Early-type Small Magellanic Cloud Eccentric Eclipsing Binaries. *AJ*, 157:87.